# The Impact of Imperfect Timekeeping on Quantum Control

Jake Xuereb, Paul Erker, Plorian Meier, Mark T. Mitchison, Marcus Huber, Vienna Center for Quantum Science and Technology, Atominstitut, TU Wien, 1020 Vienna, Austria Institute for Quantum Optics and Quantum Information (IQOQI),

Austrian Academy of Sciences, Boltzmanngasse 3, 1090 Vienna, Austria

School of Physics, Trinity College Dublin, College Green, Dublin 2, Ireland (Dated: January 26, 2023)

In order to unitarily evolve a quantum system, an agent requires knowledge of time, a parameter which no physical clock can ever perfectly characterise. In this letter, we study how limitations on acquiring knowledge of time impact controlled quantum operations in different paradigms. We show that the quality of timekeeping an agent has access to limits the gate complexity they are able to achieve within circuit-based quantum computation. It also exponentially impacts state preparation for measurement-based quantum computation. Another area where quantum control is relevant is quantum thermodynamics. In that context, we show that cooling a qubit can be achieved using a timer of arbitrary quality for control: timekeeping error only impacts the rate of cooling and not the achievable temperature. Our analysis combines techniques from the study of autonomous quantum clocks and the theory of quantum channels to understand the effect of imperfect timekeeping on controlled quantum dynamics.

Quantum control theory is an established field [1, 2] with notable successes [3], yet its basic formulation implicitly assumes that the controlling agent has perfect knowledge of time: an assumption which is never truly satisfied. Indeed, a long-standing problem in quantum theory has been to understand how resource limitations fundamentally restrict our knowledge of time [4–9]. Peres closes his seminal paper [5] with the warning "...the Hamiltonian approach to quantum physics carries the seeds of its own demise", lamenting his conclusion that controlled Hamiltonian dynamics is unachievable without access to a perfect clock requiring infinite energy. In this work, we examine whether a central task in quantum theory, that of controlled unitary operations, is limited by one's ability to tell time. In doing so, we give credence to Peres' admonition but also provide justification for the timescales over which it is fair to ignore it.

In classical computation, bits of information are abundant and their manipulation is simple. This underpins the great success of the abstract theory of classical information processing, which allows the design of algorithms without much consideration for the physical semiconductor hardware that would carry them out. Quantum computation is different: whilst any algorithm before measurement can simply be thought of as a rotation on a high-dimensional Bloch ball, such a unitary operation is necessarily generated by a time-dependent Hamiltonian. And an abstraction to perfect qubits is prohibited by the impossibility of (almost) perfect error correction, which is far more demanding for quantum information.

Characterising error, its propagation and impact is a well studied problem in quantum computation, especially within the field of randomized benchmarking [10–12]. The characterisation of these errors is robust because it is agnostic to the physical source creating them. In contrast, we focus on studying the relationship between one particular error and the physical source generating it. Specifically, we explore the error contributed by the

imperfect nature of the timekeeping device that regulates the physical control protocol, neglecting all other error sources. Our central motivation is to examine what quantum computational tasks are achievable depending on the quality of the clock one has access to. The role of timekeeping in quantum computation has been experimentally [13] and theoretically [14] investigated before, showing that it is a relevant factor in increasing the achievable quality of the computation, typically amidst other factors in a so-called error budget [15, 16] such as phase drift of the lasers in a trapped-ion setup or temperature stability in a superconducting circuit.

In this work, we use a framework for characterising the quality of timekeeping devices developed in the emerging field of autonomous quantum clocks [6-9] known as the tick distribution. A key property of a clock's tick distribution is its accuracy N, which is the expected number of "good" ticks before the clock becomes inaccurate (see Eq. (3) below for a precise definition). We show that incorporating a tick distribution within unitary time evolution enacts a dephasing channel, empowering us to use techniques developed in the characterisation of noisy channels to investigate the impact of imperfect timekeeping on quantum operations.

The main contributions we present in this letter are: firstly, that the average gate fidelity of ill-timed single-qubit and two-qubit gates obey the fidelity relation

$$\overline{\mathcal{F}}(\mathcal{D}) = \frac{2 + e^{-\frac{\theta^2}{2N}}}{3}.$$

This states that the average gate fidelity is exponentially impacted by the accuracy N of the timer, where  $\theta$  is the pulse area (i.e. the angle of rotation on an effective Bloch sphere) due to the gate. Secondly, we show that with arbitrarily imperfect timekeeping one can still cool a qubit to a desired temperature with access to asymptotically many ill-timed SWAP operations and a thermal machine.

We begin by introducing the setup for the analysis, explaining how tick distributions can be thought of in this setting and show that they impact unitary time evolution as dephasing channels. After this, we focus on the context of circuit based quantum computation, examining how imperfect timekeeping impacts the average gate fidelity of single- and two-qubit gates, where we argue that achievable gate complexity is limited by clock accuracy. Here we make the case that, given a fixed gate duration, improved timekeeping control can resolve this bottleneck. This comes at the cost of increased entropy production [7, 17, 18], dominating the dissipation associated with quantum computation and persisting even in reversible models of computation. We follow this section by discussing the task of algorithmically cooling a qubit to an arbitrary temperature using SWAP gates with access to a thermal bath [19–21] and show that whilst the resources required increase considerably, one is still able to cool to a desired temperature asymptotically, controlling this protocol with an arbitrarily imperfect clock.

Imperfect timekeeping in quantum control.—An ideal unitary quantum operation  $U=e^{-iH\tau}$  requires the ability to perfectly control the duration  $\tau$  for which we allow a physical process, generated by a Hamiltonian H, to act on a target system. One can think of this as having access to a timer which has infinite accuracy and precision in its ability to tick at a desired time and using it to control the duration of this process. In this context, imperfect timekeeping is the situation where one has access to an imperfect timer which does not always tick at the desired time to end this operation and so can result in a different unitary evolution than one expects.

We may model the quality of our timekeeping in this control process by introducing a probability distribution obtained by sampling from the timer which we are using for control. Such distributions are known as tick distributions and have been studied within the field of quantum clocks [6–9]. If the timer is perfect then we always obtain the desired duration to time our process, leading to an evolution which gives the target state

$$\rho' = \int_{-\infty}^{\infty} dt \, \delta(t - \tau) \, e^{-iHt} \rho e^{iHt}, \tag{1}$$

where  $\rho$  is the initial state and the Dirac delta function  $\delta(t-\tau)$  represents the tick distribution of an ideal timer. Instead, let us make this scenario more realistic by considering a Gaussian tick distribution, giving on average a final state of the form

$$\rho_{\text{error}}' = \int_{-\infty}^{\infty} dt \, \frac{e^{\frac{(t-\tau)^2}{-2\sigma^2}}}{\sqrt{2\pi\sigma^2}} e^{-iHt} \rho e^{iHt}, \tag{2}$$

where  $\sigma$  is the variance of the tick distribution and our desired process duration  $\tau$  is its mean. The accuracy, defined by [6–8]

$$N = \left(\frac{\tau^2}{\sigma^2}\right),\tag{3}$$

is a figure of merit ascribed to a clock which generates ticks with a temporal resolution  $\tau$  and variance  $\sigma^2$ . In this work, we focus on single-tick timers which control a gate pulse, and so the relevant clock accuracy is defined with respect to the resolution of the pulse duration,  $\tau$ .

The states  $\rho'$  and  $\rho'_{\rm error}$  are clearly not the same in general. Let the Hamiltonian be of form  $H = \sum_n E_n |n\rangle\langle n|$  so that we may express the contributions to the resultant state in the energy eigenbasis as

$$\langle n | \rho'_{\text{error}} | m \rangle = \int_{-\infty}^{\infty} dt \, \frac{e^{\frac{(t-\tau)^2}{-2\sigma^2}}}{\sqrt{2\pi\sigma^2}} \langle m | e^{-iHt} \rho e^{iHt} | n \rangle$$

$$= \int_{-\infty}^{\infty} dt \, \frac{e^{\frac{(t-\tau)^2}{-2\sigma^2}}}{\sqrt{2\pi\sigma^2}} e^{-i(E_m - E_n)t} \langle n | \rho | m \rangle$$

$$= e^{-\frac{\sigma^2}{2}(E_m - E_n)^2} e^{-i(E_m - E_n)\tau} \langle n | \rho | m \rangle \quad (4)$$

This admits two cases. For the diagonal entries m=n, the unitary has no impact on the state in the basis of its Hamiltonian generator as can be seen from (4). For the off-diagonal elements with  $m \neq n$  we see that the term  $e^{-i(E_m-E_n)\tau}$  enacts the unitary evolution in the basis of the gate Hamiltonian and the term  $e^{-\frac{\sigma^2}{2}(E_m-E_n)^2}$  causes decoherence due to the timing error. Therefore, imprecise timekeeping is described by a dephasing map over the unitary operation we are trying to carry out:

$$\rho_{\text{error}}' = \mathcal{D}\left(U\rho U^{\dagger}\right),\tag{5}$$

where  $\mathcal{D}(\cdot)$  denotes a dephasing channel in the eigenbasis of the Hamiltonian which generates U.

In Appendix A we show that Eq. (5) holds for arbitrary (non-Gaussian) tick distributions. However, in general we find that the variance alone is not sufficient to characterize the channel: the rate of dephasing depends on the full characteristic function of the tick distribution. Nevertheless, is worth pointing out that most physical timers would have a tick distribution which can be considered Gaussian as a result of the central limit theorem [22]. This is the case if evolution time  $\tau$  is actually obtained by the timer through integrating over sufficiently many shorter ticks. As such, choosing the Gaussian regime within this analysis is not overly restrictive.

Fidelity of ill-timed quantum logic gates.—The dephasing of a single qubit in a given basis is described by a channel whose Kraus operators have the form [23, 24]

$$K_1 = \sqrt{\frac{1 + e^{-\Gamma}}{2}}I$$
  $K_2 = \sqrt{\frac{1 - e^{-\Gamma}}{2}}\sigma_z$ , (6)

where  $\Gamma$  is the dephasing magnitude,  $I=|0\rangle\langle 0|+|1\rangle\langle 1|$  is the identity operator and  $\sigma_z=|0\rangle\langle 0|-|1\rangle\langle 1|$  is the operator corresponding to the population inversion in the chosen basis. In the context of Eq. (4), the states  $|0\rangle$  and  $|1\rangle$  are the eigenstates of the gate Hamiltonian, H, while  $\Gamma=\sigma^2\Omega^2/2$  with  $\Omega=E_0-E_1$  is the Rabi frequency induced on the system by the control field which mediates the gate interaction.

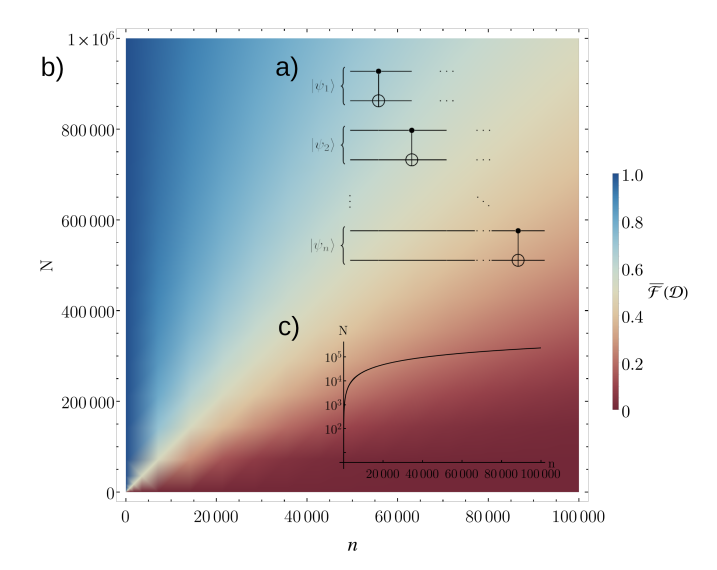


FIG. 1. For a circuit comprising n commuting gates ( $\theta=\pi$ ) such as the one shown in a), the impact of timekeeping error on average gate fidelity  $\overline{\mathcal{F}}(\mathcal{D})$  is plotted in b) as the circuit complexity increases for different values of clock accuracy N. Inset c) is the clock accuracy in logarithmic scaling against the circuit complexity for a threshold average gate fidelity of 0.5. This shows that the temporal control one has access to great impacts the gate complexity one can achieve and that this relationship is not linear.

The average gate fidelity is a measure of how much degradation a channel causes on the unitary evolution of the Haar-averaged set of qubit states for a given gate and as such presents an ideal candidate for examining the impact of imprecise timekeeping on a quantum computation. It was shown in [10, 25] that the average gate fidelity is dependent only on the noisy channel  $\mathcal{E}(\cdot) = \sum_i K_i(\cdot)K_i^{\dagger}$  being considered as  $\overline{\mathcal{F}}(\mathcal{E}) = \frac{\sum_i |\operatorname{tr} K_i|^2 + d}{d^2 + d}$ , where d is the dimension of the Hilbert space we are averaging over. Applying this expression to our dephasing channel we obtain the average gate fidelity

$$\overline{\mathcal{F}}(\mathcal{D}) = \frac{2 + e^{-\frac{\theta^2}{2N}}}{3},\tag{7}$$

expressed in terms of the pulse area  $\theta = \Omega \tau$  and the accuracy defined in Eq. (3). Eq. (7) exposes the exponential impact of clock accuracy on gate fidelity. Note that this impact is dependent on the size of the rotation on the Bloch ball related to the gate, such that larger rotations are more susceptible to being impacted by the quality of timekeeping.

We can extend this result to the CNOT gate which, when combined with single qubit rotations, forms a universal gate set [26]. The CNOT can be generated by a Hamiltonian that only acts on the subspace spanned by  $|10\rangle$ ,  $|11\rangle$  allowing us to consider this operation as acting on an effective qubit with basis states  $|10\rangle$ ,  $|11\rangle$ . The impact of imperfect timekeeping will be dephasing within this non-local subspace. The resultant average gate fi-

delity of ill-timed two qubit entangling gates is therefore given by Eq. (7) with  $\theta=\pi$ . This generalisation is explored in further detail in Appendix B 1.

A measure of the circuit complexity of a unitary operation is its CNOT count. It is interesting to then ask what circuit complexity is achievable with access to a given quality of timekeeping resource. This question is not straightforward to investigate as the impact of timekeeping error on a circuit is highly dependent on its structure. As a first step, we consider circuits comprising gates which commute with each other. An example is the circuit where n CNOTs are applied in parallel to m = 2n qubits (see Fig. 1 a)). This circuit can be used, for example, to generate n Bell pairs as a resource for quantum cryptography [27, 28]. Another example is the circuit that generates a 2D cluster state in preparation for measurement based quantum computation [29], which involves  $n = m^2$  controlled-Z operations applied to m qubits. Such circuits would have an average gate

fidelity  $\overline{\mathcal{F}} = \left(\frac{2+e^{-\frac{\theta^2}{2N^2}}}{3}\right)^n$  due to the commutativity of the Kraus operators when concatenating the same chan-

the Kraus operators when concatenating the same channel. We plot this relationship for different values of the timing accuracy in Figure 1. Note that the specific applications mentioned above — namely, the creation of Bell pairs or a 2D cluster state — require the particular input state  $|+\rangle^{\otimes m}$ , for which the fidelity scaling would be even worse than the average gate fidelity shown in Fig. 1.

For more general circuits with non-commuting gates, one might be tempted to think that different errors due to timekeeping could counteract each other. But we find that they can conspire to effect a fidelity scaling that is even worse than the commuting case. For such an example, consider the 7 qubit gate decomposition of the Toffoli gate, which acts as the diffusion operator for the Grover algorithm on 3 qubits [30, 31]. We see in Figure 2 that the average fidelity for the Toffoli gate is strictly worse than that of 7 CNOTs acting in a commuting fashion. This is explored in further depth in Appendix B 3.

To estimate the quantitative impact of imperfect timekeeping on quantum computation, we can consider some rough estimates. Setting an average gate fidelity threshold at 0.5 for the entire computation, Eq. (7) suggests that we can execute a circuit such as Fig 1 a) featuring  $n = 1 \times 10^6$  CNOTs given a clock accuracy of  $N=1\times 10^6$ . At the same fidelity threshold,  $n=1\times 10^4$ CNOTs are achievable with a clock accuracy of N = $2.5 \times 10^4$ , as shown in Fig. 1 c). This circuit complexity is consistent with state-of-the-art benchmarking algorithms, where CNOT gates may number in the tens of thousands [32]. Considering a gate duration of  $\tau = 100$ ns, these accuracies would correspond to timing uncertainties of  $\sigma = 0.1$  ns and  $\sigma \approx 0.633$  ns, respectively. Modern control systems such as the ARTIQ Sinara suffer from electronic jitter of 0.3 ns, signalling that timekeeping is still a limiting factor for experiments. However, typical experimental error budgets [16, 33] include other timekeeping errors beyond jitter, including the frequency

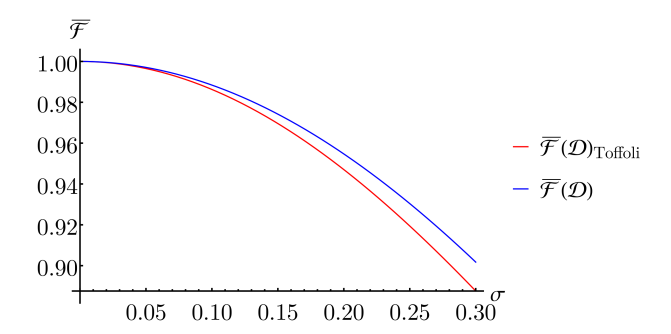


FIG. 2. A comparison of the average fidelity decay between the 7 gate implementation of the Toffoli gate and 7 CNOT gates carried out consecutively, for different values of uncertainty in timekeeping  $\sigma$  and fixed  $\tau$  for the timer controlling the Hamiltonian evolution.

instability of local oscillators [13] and peak disortion in their signal. This leads us to believe that the identification and quantification of all sources contributing to experimental timekeeping uncertainty remains an important task. Doing so would help to connect the physics of quantum control with recent theoretical progress in the foundations of timekeeping [6–9].

Imperfect timekeeping is sufficient for cooling.—Our results so far corroborate an accepted wisdom in the practice of quantum computation: timing operations precisely and fast is a key technological challenge that will have to be met for fault-tolerant quantum computation [34–36]. This being said, controlled unitary operations also appear in more conceptual areas of quantum theory, e.g. in quantum thermodynamics. In that context, the ramifications of imperfect timekeeping have only recently begun to come to light [37–39]. As a concrete thermodynamic protocol, we consider algorithmic cooling [20, 21, 40, 41], where a series of controlled unitary operations is used to perform refrigeration. Such protocols can be broken down into SWAP-inducing interactions enacted between the energy levels of a thermal machine and the system to be cooled. In [19], the achievability of this cooling protocol is shown for the task of cooling a qubit to any desired temperature given access to an appropriate thermal machine, whilst bounds on its performance were obtained in [21].

**Theorem 1.** A qubit in a thermal state at temperature  $\beta_s$  with ground state population  $r_s$  can be asymptotically cooled to a thermal state with ground state population  $r_v: r_v > r_s$  and inverse temperature  $\beta_v: \beta_v > \beta_s$  in a protocol controlled by a timer with a Gaussian tick distribution with mean  $\tau$  and variance  $\sigma$ .

Here is a sketch of the proof. A pair of energy levels of the thermal machine are chosen, such that the subspace they form can be thought of as a virtual qubit with inverse temperature  $\beta_v: \beta_v > \beta_s$ . The probability that this subspace is populated is  $P_v: 0 < P_v < 1$ , which is less than unity because the machine may have many levels. To cool the physical qubit, the agent attempts

to generate a SWAP operation between the virtual and physical qubits by enacting a Hamiltonian for a time  $\tau$  using a timer with finite accuracy N. The imperfect timer dephases this operation, resulting in the ground state population of the virtual qubit being only partially swapped with that of the physical qubit. Attempting to apply n SWAPs recursively, the agent manages to change the ground state population of the physical qubit to

$$r_{\text{error}}^{(n)} = r_v - (r_v - r_s)(1 - P_v(1 - p))^n, \tag{8}$$

where  $p = \frac{1}{2} \left( 1 - e^{-\frac{\pi^2}{2N}} \right)$  appears due to the imperfect temporal control. Asymptotically as  $n \to \infty$ ,  $r_{\rm error}^{(n)}$  converges to  $r_v$ , i.e. the physical qubit converges to a thermal state with the target temperature  $\beta_v$ , regardless of the control timer's uncertainty  $\sigma$ . Whilst imperfect time-keeping is sufficient for an agent to cool a qubit to a desired temperature, there is a cost in terms of the number of operations required, which scales inversely with the accuracy of the timer. We examine how  $\sigma$  impacts the rate of cooling in this protocol in Appendix C.

Discussion.—In this work we have shown that Peres' concern is not only relevant to the foundations of quantum theory but also to operational tasks such as computation and refrigeration. Within the context of our model, Figure 1 shows that quantum algorithms with different circuit complexity are achievable depending on clock accuracy and that this relationship is nonlinear. The clock accuracy an agent has access to is a ratio between the duration of the protocol and the uncertainty in their timing. This suggests that, for a given timing uncertainty, carrying out a longer operation allows one to obtain a higher fidelity, which is reminiscent of the accuracy-resolution trade-off for clocks examined recently in Ref. [42].

Our quantitative estimates indicate that, for experimentally relevant gate counts and durations, imperfect timekeeping may become a significant error source when the timing uncertainty  $\sigma$  is on the picosecond scale or greater. It is crucial to emphasise that this is the uncertainty in timing the duration of each quantum gate, which must necessarily be very fast (e.g. nanoseconds) in order to counteract environment-induced decoherence. Precise timing of such short time intervals remains an outstanding technical challenge. This should be contrasted with the sub-femtosecond uncertainty of atomic clocks, which is only achieved after integration times of seconds, hours or several days [43] depending on the system.

From a foundational perspective, our results have serious implications for the thermodynamics of quantum computation. Several papers explore this question focusing only on the energetics of the system itself [44–48]. While it is obvious that current technologies are dominated by the classical control size (refrigeration and laser pulses), there is hope in the community that, once larger circuits can be fit into those same fridges and reversible computation is possible, there will be an ener-

getic advantage to quantum computation. By considering a single source of error we show that there is an intrinsic requirement that cannot be overcome and which scales with the circuit depth: the need for precise and accurate timekeeping for every gate. Yet mounting evidence — underpinned by the discovery of thermodynamic uncertainty relations [49-51] — demonstrates that precise timekeeping generally comes at a thermodynamic cost [7, 9, 17, 18] (although see Ref. [52] for a classical counterexample). For the autonomous thermal clocks considered in [7, 9, 17], the accuracy N is shown to be bounded from above by

$$N \le \frac{\Delta S_{\text{tick}}}{2}.\tag{9}$$

where  $\Delta S_{\rm tick}$  is the entropy produced by the clock to generate each tick. This entropy production entails heat dissipation into the environment, implying that the contribution to the energetic cost of a quantum computation derived from the physics of timed quantum control cannot be ignored. Indeed, to achieve fault tolerance [34–36], each logical qubit will be made of a large number of physical qubits and thus every error correction step will incur increased costs on the level of control.

A thorough analysis of the growth of timekeeping error for arbitrary circuits and gate sets was out of scope for this work, because characterising the impact of concatenated channels on average gate fidelity is non-trivial

as discussed in Appendix B 3. Techniques like channel approximation for composite channels [12] suggest a possible route for further examination.

It might seem that the message of this work is pessimistic, but the fact that timing is an issue in quantum computation is not unknown to those building physical devices. Algorithms have been developed in the field of optimal quantum control [53–55] where bulk errors can be mitigated by cleverly and dynamically changing a control field's frequency throughout the duration of a pulse. We expect that, by characterising the physics of specific sources of error within quantum computation as we have attempted in this work, analytical strategies to combat their errors within the field of optimal quantum control can be conceived.

Acknowledgements.—The authors thank Parnam (Faraj) Bakhshinezhad, Steve Campbell and Phila Rembold for insightful discussions. We especially thank Martin Ringbauer for sharing his knowledge of the state of the art of timing resolution in modern quantum control. J.X. and M.H. would like to acknowledge funding from the European Research Council (Consolidator grant 'Cocoquest' 101043705). F.M., M.T.M and M.H. further acknowledge funding by the European flagship on quantum technologies ('ASPECTS' consortium 101080167). P.E. and M.H. further acknowledge funds from the FQXi (FQXi-IAF19-03-S2) within the project "Fueling quantum field machines with information". M.T.M.is supported by a Royal Society-Science Foundation Ireland University Research Fellowship.

H. M. Wiseman and G. J. Milburn, *Quantum Measure-ment and Control*, 1st ed. (Cambridge University Press, 2009).

<sup>[2]</sup> S. Cong, Control of quantum systems: theory and methods (John Wiley & Sons Inc, Singapore, 2014).

<sup>[3]</sup> C. P. Koch, U. Boscain, T. Calarco, G. Dirr, S. Filipp, S. J. Glaser, R. Kosloff, S. Montangero, T. Schulte-Herbrüggen, D. Sugny, and F. K. Wilhelm, EPJ Quantum Technology 9, 19 (2022).

<sup>[4]</sup> H. Salecker and E. P. Wigner, Phys. Rev. 109, 571 (1958).

<sup>[5]</sup> A. Peres, American Journal of Physics 48, 552 (1980).

<sup>[6]</sup> M. P. Woods, R. Silva, and J. Oppenheim, Annales Henri Poincaré 20, 125 (2019).

<sup>[7]</sup> P. Erker, M. T. Mitchison, R. Silva, M. P. Woods, N. Brunner, and M. Huber, Phys. Rev. X 7, 031022 (2017).

<sup>[8]</sup> M. P. Woods, Quantum 5, 381 (2021).

<sup>[9]</sup> E. Schwarzhans, M. P. E. Lock, P. Erker, N. Friis, and M. Huber, Phys. Rev. X 11, 011046 (2021).

<sup>[10]</sup> J. Emerson, R. Alicki, and K. Życzkowski, Journal of Optics B: Quantum and Semiclassical Optics 7, S347 (2005).

<sup>[11]</sup> E. Magesan, J. M. Gambetta, and J. Emerson, Physical Review Letters 106 (2011), 10.1103/physrevlett.106.180504.

<sup>[12]</sup> A. Carignan-Dugas, K. Boone, J. J. Wallman, and J. Emerson, New Journal of Physics 20, 092001 (2018).

<sup>[13]</sup> H. Ball, W. D. Oliver, and M. J. Biercuk, npj Quantum Information 2 (2016), 10.1038/npjqi.2016.33.

<sup>[14]</sup> X. Jiang, J. Scott, M. Friesen, and M. Saffman, "Sensitivity of quantum gate fidelity to laser phase and intensity noise," (2022), arXiv:2210.11007 [quant-ph].

<sup>[15]</sup> C. J. Ballance, T. P. Harty, N. M. Linke, M. A. Sepiol, and D. M. Lucas, Phys. Rev. Lett. 117, 060504 (2016).

<sup>[16]</sup> P. Hrmo, B. Wilhelm, L. Gerster, M. W. van Mourik, M. Huber, R. Blatt, P. Schindler, T. Monz, and M. Ringbauer, "Native qudit entanglement in a trapped ion quantum processor," (2022).

<sup>[17]</sup> A. C. Barato and U. Seifert, Phys. Rev. X 6, 041053 (2016).

<sup>[18]</sup> A. N. Pearson, Y. Guryanova, P. Erker, E. A. Laird, G. A. D. Briggs, M. Huber, and N. Ares, Phys. Rev. X 11, 021029 (2021).

<sup>[19]</sup> R. Silva, G. Manzano, P. Skrzypczyk, and N. Brunner, Physical Review E 94 (2016), 10.1103/physreve.94.032120.

<sup>[20]</sup> F. Clivaz, R. Silva, G. Haack, J. B. Brask, N. Brunner, and M. Huber, Physical Review E 100 (2019), 10.1103/physreve.100.042130.

<sup>[21]</sup> F. Clivaz, R. Silva, G. Haack, J. B. Brask, N. Brunner, and M. Huber, Physical Review Letters 123 (2019), 10.1103/physrevlett.123.170605.

<sup>[22]</sup> A. Klenke, *Probability Theory* (Springer International Publishing, 2020).

- [23] H.-P. Breuer and F. Petruccione, *The Theory of Open Quantum Systems* (Oxford University Press, 2007).
- [24] B. Bylicka, D. Chruściński, and S. Maniscalco, Scientific Reports 4 (2014), 10.1038/srep05720.
- [25] M. A. Nielsen, Physics Letters A 303, 249 (2002).
- [26] M. A. Nielsen and I. L. Chuang, Quantum Computation and Quantum Information: 10th Anniversary Edition (Cambridge University Press, 2010).
- [27] A. K. Ekert, Phys. Rev. Lett. 67, 661 (1991).
- [28] C. H. Bennett, G. Brassard, and N. D. Mermin, Phys. Rev. Lett. 68, 557 (1992).
- [29] R. Raussendorf and H. J. Briegel, Phys. Rev. Lett. 86, 5188 (2001).
- [30] C. Figgatt, D. Maslov, K. A. Landsman, N. M. Linke, S. Debnath, and C. Monroe, Nature Communications 8 (2017), 10.1038/s41467-017-01904-7.
- [31] K. Zhang and V. E. Korepin, Physical Review A 101 (2020), 10.1103/physreva.101.032346.
- [32] M. Amy, P. Azimzadeh, and M. Mosca, Quantum Science and Technology 4, 015002 (2018).
- [33] V. M. Schäfer, C. J. Ballance, K. Thirumalai, L. J. Stephenson, T. G. Ballance, A. M. Steane, and D. M. Lucas, Nature 555, 75–78 (2018).
- [34] D. Aharonov and M. Ben-Or, in Proceedings of the twenty-ninth annual ACM symposium on Theory of computing - STOC '97 (ACM Press, 1997).
- [35] S. Bravyi and A. Kitaev, Phys. Rev. A 71, 022316 (2005).
- [36] E. Knill, R. Laflamme, and W. H. Zurek, Proceedings of the Royal Society of London. Series A: Mathematical, Physical and Engineering Sciences 454, 365 (1998).
- [37] A. S. L. Malabarba, A. J. Short, and P. Kammerlander, New Journal of Physics 17, 045027 (2015).
- [38] M. P. Woods and M. Horodecki, "The resource theoretic paradigm of quantum thermodynamics with control," (2019), arXiv:1912.05562 [quant-ph].
- [39] P. Taranto, F. Bakhshinezhad, A. Bluhm, R. Silva, N. Friis, M. P. E. Lock, G. Vitagliano, F. C. Binder, T. Debarba, E. Schwarzhans, F. Clivaz, and M. Huber, "Landauer vs. nernst: What is the true cost of cooling a quantum system?" (2021), arXiv:2106.05151v2 [quantph].
- [40] D. K. Park, N. A. Rodriguez-Briones, G. Feng, R. Rahimi, J. Baugh, and R. Laflamme, Electron Spin Resonance (ESR) Based Quantum Computing, 227 (2016).
- [41] E. Bäumer, M. Perarnau-Llobet, P. Kammerlander, H. Wilming, and R. Renner, Quantum 3, 153 (2019).
- [42] F. Meier, E. Schwarzhans, P. Erker, and M. Huber, "Fundamental accuracy-resolution trade-off for timekeeping devices," (2023).
- [43] X. Zheng, J. Dolde, V. Lochab, B. N. Merriman, H. Li, and S. Kolkowitz, Nature 602, 425 (2022).
- [44] M. Amoretti, Quantum Views 5, 52 (2021).
- [45] S. Deffner, Europhysics Letters **134**, 40002 (2021).
- [46] J. Stevens, D. Szombati, M. Maffei, C. Elouard, R. Assouly, N. Cottet, R. Dassonneville, Q. Ficheux, S. Zeppetzauer, A. Bienfait, A. Jordan, A. Auffèves, and B. Huard, Physical Review Letters 129 (2022), 10.1103/physrevlett.129.110601.
- [47] G. Chiribella, Y. Yang, and R. Renner, Physical Review X 11 (2021), 10.1103/physrevx.11.021014.
- [48] G. Chiribella, F. Meng, R. Renner, and M.-H. Yung, Nature Communications 13 (2022), 10.1038/s41467-022-34541-w.

- [49] A. C. Barato and U. Seifert, Phys. Rev. Lett. 114, 158101 (2015).
- [50] T. R. Gingrich, J. M. Horowitz, N. Perunov, and J. L. England, Phys. Rev. Lett. 116, 120601 (2016).
- [51] J. M. Horowitz and T. R. Gingrich, Nature Physics 16, 15 (2020).
- [52] P. Pietzonka, Phys. Rev. Lett. 128, 130606 (2022).
- [53] P. Rembold, N. Oshnik, M. M. Müller, S. Montangero, T. Calarco, and E. Neu, AVS Quantum Science 2, 024701 (2020).
- [54] J.-S. Li, J. Ruths, T.-Y. Yu, H. Arthanari, and G. Wagner, Proceedings of the National Academy of Sciences 108, 1879 (2011).
- [55] S. Machnes, U. Sander, S. J. Glaser, P. de Fouquières, A. Gruslys, S. Schirmer, and T. Schulte-Herbrüggen, Physical Review A 84 (2011), 10.1103/physreva.84.022305.
- [56] A. Barenco, C. H. Bennett, R. Cleve, D. P. DiVincenzo, N. Margolus, P. Shor, T. Sleator, J. A. Smolin, and H. Weinfurter, Physical Review A 52, 3457 (1995).
- [57] Note that we may use the same dephasing channel to examine the impact of the rotation gate and its Hermitian conjugate because they share the same energy eigenbasis and so are dephased in the same subspace.

#### **APPENDICES**

### Appendix A: The Impact of Arbitrary Tick Distributions on Unitary Time Evolution

Equation (4) is the specific expression for the time-evolution of the density matrix in case that the tick waiting time is Gaussian distributed. While in a first approximation this may be justified, it is to be expected, that in general the waiting time distribution for a tick is not Gaussian [6, 9]. Exponential decay for example is not Gaussian, but a primitive example for a thermal clock. To generalize the dephasing result from eq. (4), let us introduce a general tick probability density p(t). For the sake of the argument, let us assume that aside from being normalized, both the first  $t_1$  and second moment  $t_2$  of p(t) exist. In the usual notation, we have

$$\tau \equiv t_1$$
, and  $\sigma^2 \equiv t_2 - t_1^2$ . (A1)

The matrix element (m, n) of the density matrix  $\rho$  after the unitary evolution (with unsharp timing) is given by an analogous expression as eq. (4),

$$\tilde{\rho}_{m,n} = \int_{-\infty}^{\infty} dt p(t) e^{-i(E_m - E_n)t} \rho_{m,n} \tag{A2}$$

$$= \rho_{m,n} e^{-i(E_m - E_n)\tau} \int_{-\infty}^{\infty} dt p(t - \tau) e^{-i(E_m - E_n)t}$$
(A3)

$$= \rho_{m,n} e^{-i(E_m - E_n)\tau} \varphi_{T_\tau p}(E_m - E_n). \tag{A4}$$

From eq. (A3) to eq. (A4), we have abbreviated the Fourier transform of the shifted probability density function  $T_{\tau}p(t) := p(t-\tau)$ . The expression  $\varphi_{T_{\tau}p}(\Omega)$  is known as the characteristic function of the probability density  $T_{\tau}p$  [22]. The contribution from the first moment of the tick probability density p(t) has been factored out by means of a variable change. As a result, the unitary evolution factor  $e^{-i\Omega t}$  is present in eq. (A4) and all the dephasing contributions are within the characteristic function  $\varphi$ . In a next step we would like to give a more concrete characterization of the magnitude of the dephasing based on the uncertainty of the original tick distribution. What we would expect is that a narrow tick time distribution (that is,  $\sigma^2$  is vanishing) gives rise to little dephasing, as this case asymptotically coincides with perfect time-keeping (and thus unitary evolution). Conversely, for a tick distribution with large uncertainty  $\sigma$  in the time of arrival of the control clock's tick, we would expect stronger dephasing. The strength of the dephasing is given by the magnitude of  $\varphi(\Omega)$  (subscript implicit from now on). An additional complex phase in  $\varphi(\Omega)$  is also possible if p is not symmetric around  $\tau$ . The dephasing rate  $\Gamma$  from the main text can be obtained as

$$\Gamma = -\log|\varphi(\Omega)|,\tag{A5}$$

for a Rabi pulse inducing a frequency  $\Omega$ . In the general case again, the two functions  $\varphi(\Omega)$  and p(t) are related by a Heisenberg-type uncertainty relation coming from the Fourier conjugation of the pair  $(\Omega, t)$ . One would expect a narrow distribution in time-domain of the tick probability density p(t) to yield a wide distribution in energy-domain, that is  $\varphi(\Omega)$  drops slowly. Consequently, for sharp tick distributions we would have little dephasing. The other way around, a wide distribution in time-domain gives a narrow energy-domain distribution, meaning  $\varphi(\Omega)$  drops off quickly and the dephasing is relevant already for pulses addressing small transitions inducing a frequency  $\Omega$ .

A counterexample. One may be tempted to conclude that a tick distribtion p(t) with some variance  $\sigma^2 > 0$  results in a lower bound for the amount of dephasing, given by  $\varphi(\Omega) \leq g(\Omega, \sigma) < 1$ . The term g is some function that can be expressed in terms of the tick time uncertainty and energy gap  $\Omega = E_m - E_n$ . There are pathological, comb-like tick probability distributions, for which such a statement is false. Take the distribution

$$p(t) = \frac{1}{n} \sum_{k=0}^{n-1} \delta\left(t - \frac{k}{n\epsilon}\right). \tag{A6}$$

This distribution describes an imperfect clock in the sense that it has non-zero variance,  $\sigma > 0$ . It describes a time-keeping device whose tick happens at multiples of  $1/n\epsilon$ , with equal probability 1/n. The characteristic function is

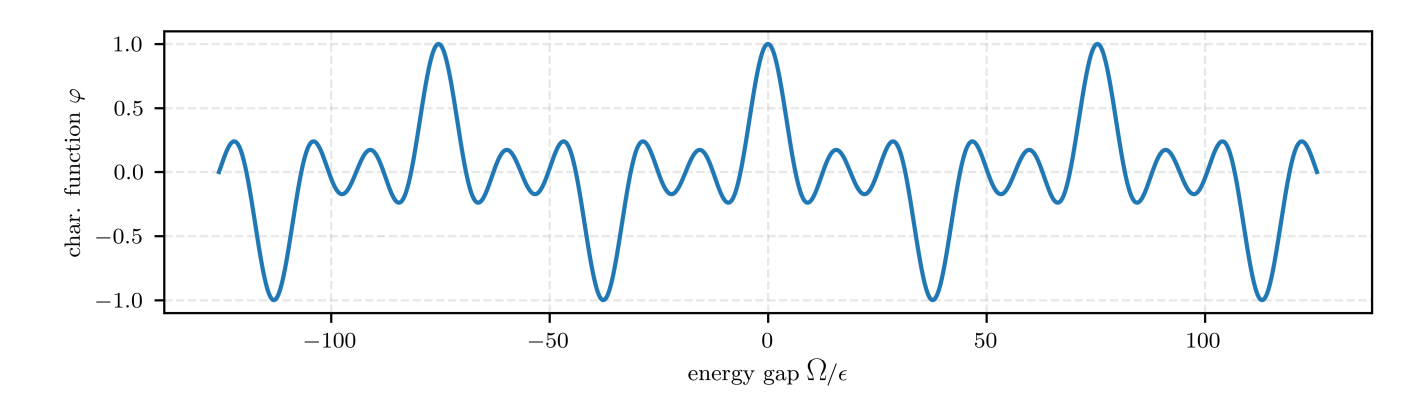


FIG. 3. This plot shows the pathological characteristic function from eq. (A9). This example illustrates that there exist (non-Gaussian) tick probability densities whose dephasing rate  $\Gamma$  does not diverge for large Rabi frequencies  $\Omega$ . The x-axis shows the values of  $\Omega/\epsilon$  and the y-axis the value of  $\varphi(\Omega)$  up to the global complex phase. It shows a dephasing function that periodically reaches unit magnitude, providing an example that even with **imperfect timekeeping**, that is  $\sigma > 0$ , it is possible to have certain off-diagonal elements that **do not dephase** for given values of  $E_n - E_m \neq 0$ .

given by the expression

$$\varphi(\Omega) = \frac{1}{n} \sum_{k=0}^{n-1} e^{-i\frac{\Omega}{\epsilon} \frac{k}{n}}$$
(A7)

$$=\frac{1}{n}\frac{1-e^{-i\frac{\Omega}{\epsilon}}}{1-e^{-i\frac{\Omega}{n\epsilon}}}\tag{A8}$$

$$= \frac{e^{-i\frac{\Omega}{\epsilon}\left(\frac{1}{2} + \frac{1}{2n}\right)}}{n} \frac{\sin(\Omega/2\epsilon)}{\sin(\Omega/2n\epsilon)}.$$
 (A9)

Ignoring the global phase which comes from the fact that p(t) does not have average  $\tau = 0$ , we obtain a function which periodically reaches unity when  $\Omega$  is a multiple of  $n\varepsilon$  (see Figure 3).

#### Appendix B: Infidelity Relationships

### 1. Average Channel Fidelity for a CNOT with imperfect timekeeping

In the computational basis the CNOT gate can be expressed as

$$CNOT = |00\rangle\langle 00| + |01\rangle\langle 01| + |1+\rangle\langle 1+| - |1-\rangle\langle 1-|$$
(B1)

and so can be expressed in terms of the matrix exponential of its generator as

$$CNOT = e^{-i|1-\rangle\langle 1-|\pi|}.$$
 (B2)

Here,  $|1-\rangle\langle 1-|$  may be considered the Hamiltonian of the process carried out to enact CNOT with  $\tau=\pi$  being its duration. This generator only acts on the  $|10\rangle$ ,  $|11\rangle$  subspace allowing us to consider this operation as one acting on an effective single qubit whose basis states are  $|10\rangle$  and  $|11\rangle$ . In this subspace, temporal error will affect the computation as follows

$$\rho_{\text{error}}' = \int_{-\infty}^{\infty} \frac{1}{\sqrt{2\pi\sigma^2}} e^{\frac{(t-\pi)^2}{-2\sigma^2}} e^{-i|1-\rangle\langle 1-|t|} \rho e^{-i|1-\rangle\langle 1-|t|} dt.$$
 (B3)

Diagonalising  $|1-\rangle\langle 1-|$  in this effective one qubit subspace, we may determine the basis in which the dephasing will occur and so the Kraus operators corresponding to a time error channel for this operation. The states  $|+'\rangle = \frac{|10\rangle + |11\rangle}{\sqrt{2}}$ 

and  $|-'\rangle = \frac{|10\rangle - |11\rangle}{\sqrt{2}}$  diagonalise this Hamiltonian meaning that the operation is equivalent to  $\sigma_x$  carried out on this effective single qubit which we can express as

$$\sigma_r' = |+'\rangle\langle +'| - |-'\rangle\langle -'|. \tag{B4}$$

As a result we can apply the single qubit dephasing model from earlier to the subspace of this non-local qubit giving

$$K_{1} = \sqrt{\frac{1 + e^{-\frac{\sigma^{2}\Omega^{2}}{2}}}{2}} I_{1} \oplus (|+'\rangle\langle +'| + |-'\rangle\langle -'|)$$

$$K_{2} = \sqrt{\frac{1 - e^{-\frac{\sigma^{2}\Omega^{2}}{2}}}{2}} I_{1} \oplus (|+'\rangle\langle +'| - |-'\rangle\langle -'|)$$
(B5)

where  $\Omega$  is the effective Rabi frequency induced by the control field on the the non-local qubit with basis states  $|+'\rangle$ ,  $|-'\rangle$ , allowing us to obtain the infidelity relation

$$\overline{\mathcal{F}}(\mathcal{D}) = \frac{1}{3} \left( 2 + e^{\frac{-\sigma^2 \Omega^2}{2}} \right) \tag{B6}$$

which has the same form as eq. 7.

### 2. Imperfect Timekeeping on the SWAP Operation

Similarly to CNOT, the SWAP operation can also be seen to act on a non-local single qubit subspace. In the Pauli Gate basis, the SWAP gate can be expressed as

$$SWAP = \frac{1}{2} (I \otimes I + X \otimes X + Y \otimes Y + Z \otimes Z)$$
(B7)

meaning that we may rewrite this as the matrix exponential

$$SWAP = e^{-i|\Psi^-\rangle\langle\Psi^-|\pi}$$
(B8)

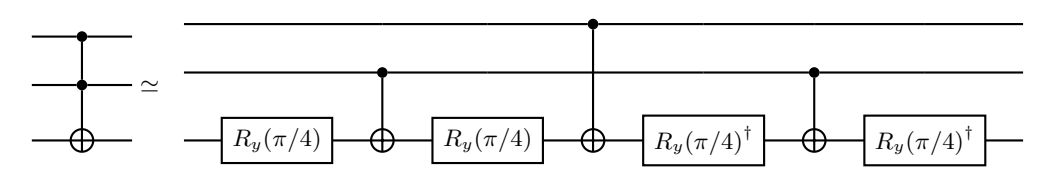
where  $|\Psi^{-}\rangle = \frac{|01\rangle - |10\rangle}{\sqrt{2}}$  is one of the Bell basis states. As such the generator of the SWAP gate acts on the non-local virtual single qubit subspace spanned by  $|\Psi^{+}\rangle$  and  $|\Psi^{-}\rangle$ . Therefore, in the same spirit as the derivation in B1 imperfect timekeeping of the SWAP gate is given by a dephasing channel with Kraus operators

$$K_1 = \sqrt{\frac{1 + e^{-\frac{\sigma^2 \Omega^2}{2}}}{2}} I_1 \oplus \left( |\Psi^+\rangle\langle \Psi^+| + |\Psi^-\rangle\langle \Psi^-| \right) \qquad K_2 = \sqrt{\frac{1 - e^{-\frac{\sigma^2 \Omega^2}{2}}}{2}} I_1 \oplus \left( |\Psi^+\rangle\langle \Psi^+| - |\Psi^-\rangle\langle \Psi^-| \right)$$
(B9)

where  $\Omega$  is the Rabi frequency induced on the virtual qubit with basis states  $|\Psi^{+}\rangle$ ,  $|\Psi^{-}\rangle$ .

## 3. Impact of Concatenated Imperfect Timekeeping in a Quantum Circuit - Toffoli

The nontrivial horizontal scaling of the impact of imperfect timekeeping on average gate fidelity, is not straightforward to analyse. In a generalised setting since the Kraus operators of the concatenation of n dephasing channels are  $2^n$  Kraus operators given by the direct product  $\{K_1, K_2\}^{\times n}$ . This results in the average gate fidelity being computationally intractable in n. To give a sense for how the impact of imperfect timekeeping would scale throughout an algorithm we examine its growth in the implementation of the three qubit Grover diffusion operator allowing us to compare with experimental results [30]. The three qubit Grover diffusion operator is simply the Toffoli gate [31] which we can be implemented up to a phase through the provably optimal gate decomposition [56] given below. To



investigate how timekeeping error would impact this implementation we consider 7 concatenated dephasing channels

representing each step in the above circuit. From the perspective of timekeeping there are 3 situations [57], (A) a y-rotation gate on the the 3rd qubit, a controlled not gate across the 2nd and 3rd qubits (B) and a controlled not gate across the 1st and 3rd qubits (C). This gives three dephasing channels  $\mathcal{D}(R_y(\pi/4))$ ,  $\mathcal{D}(\text{CNOT}_{23})$  and  $\mathcal{D}(\text{CNOT}_{13})$  which can be represented as in previous sections each with two Kraus operators say  $A_1, A_2, B_1, B_2$  and  $C_1, C_2$ . This would give a total dephasing channel for the whole protocol with 128 Kraus operators of form

$$K_{i,j,k,l,m,n,o} = A_o B_n A_m C_l A_k B_j A_i : i, j, k, l, m, n, o \in \{1, 2\}.$$
 (B10)

which we then use to calculate the average gate fidelity for this composite imperfect timekeeping channel which is plotted in Fig. 2. Here we see that the non-commuting errors in this implementation of the Toffoli gate do not in general cancel eachother out to give an improved fidelity decay relation but instead compound giving one which is worse than that of a circuit of commuting CNOTs as described in the main text. This suggests that an in-depth analysis of the impact of imperfect timekeeping both by classifying the errors that different clocks can impart and how the error they impart scales in various quantum algorithms is a promising avenue for future investigations.

#### Appendix C: An Imperfectly Timed Cooling Protocol

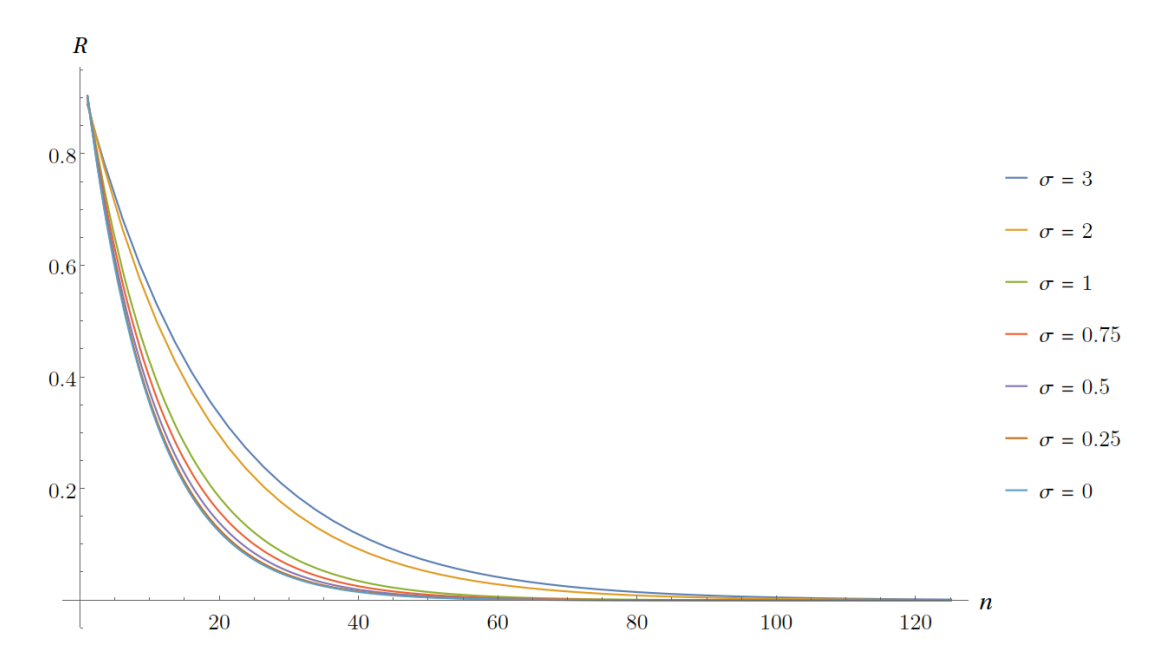


FIG. 4. The rate of cooling, given by a central difference with step h=0.1, against the number of SWAPs carried out in the protocol for different imperfect timekeeping control expressed by  $\sigma$  the variance of the tick distribution. In each plot the virtual qubit occupation  $P_v=0.1$ , target ground state population  $r_v=0.999$ , initial qubit ground state population  $r_s=0.5$  were fixed, with only  $\sigma$  varying.

Assume that the physical qubit is in an initial thermal state  $\rho_s$  at inverse temperature  $\beta$  with Hamiltonian  $H = -\omega_s \sigma_z$  giving

$$\rho_s = \frac{1 + Z_s}{2} |0\rangle\langle 0|_s + \frac{1 - Z_s}{2} |1\rangle\langle 1|_s \tag{C1}$$

where  $Z_s = \tanh(\beta \omega_s)$  is the partition function. The state of the machine is

$$\rho_v = P_v \left( \frac{1 + Z_v}{2} |i\rangle\langle i|_v + \frac{1 - Z_v}{2} |j\rangle\langle j| \right) + (1 - P_V) \tilde{\rho}_v \tag{C2}$$

where  $P_v = p_i + p_j < 1$  is the sum of the occupation of the energy levels of this ladder system which we are using to define our virtual qubit and  $\tilde{\rho_v}$  is the state of the rest of the ladder system. Here the partition function is given by

 $Z_v = \tanh(\beta_v \Delta)$  where  $\Delta = E_j - E_i$  and  $\beta_v$  is the virtual qubit temperature. Enacting the SWAP operation to cool the system results in

$$\rho' = \text{SWAP}\rho_s \otimes \rho_v \text{SWAP} = \left(\frac{1+Z_s}{2}\right) P_v \left(\frac{1+Z_v}{2}\right) |00\rangle\langle 00|_{sv} + \left(\frac{1-Z_s}{2}\right) P_v \left(\frac{1+Z_v}{2}\right) |01\rangle\langle 01|_{sv} + \left(\frac{1+Z_s}{2}\right) P_v \left(\frac{1-Z_v}{2}\right) |10\rangle\langle 10|_{sv} + \left(\frac{1-Z_s}{2}\right) P_v \left(\frac{1-Z_v}{2}\right) |11\rangle\langle 11|_{sv} + (1-P_V) \rho_s \otimes \tilde{\rho}_v \quad (C3)$$

and the reduced system state

$$\rho_s' = \left[ P_v \left( \frac{1 + Z_v}{2} \right) + (1 - P_V) \left( \frac{1 + Z_s}{2} \right) \right] |0\rangle \langle 0|_s + \left[ P_v \left( \frac{1 - Z_v}{2} \right) + (1 - P_V) \left( \frac{1 - Z_s}{2} \right) \right] |1\rangle \langle 1|_s. \tag{C4}$$

This implies that we may relate the normalised ground state probabilities as

$$r_s' = P_v r_v + (1 - P_v) r_s$$
 (C5)

that is with probability  $P_v$  we have the ground state probability of the virtual qubit and with probability  $(1 - P_v)$  we have the initial ground state probability. With time error of tick variance  $\sigma$  we instead have

$$\rho'_{\text{error}} = \mathcal{D}\left(\text{SWAP}\rho_s \otimes \rho_v \text{SWAP}\right) \tag{C6}$$

$$= \left(\frac{1+Z_s}{2}\right) P_v \left(\frac{1+Z_v}{2}\right) |00\rangle\langle 00|_{sv} + \frac{P_v}{4} \left(1-Z_s Z_v + e^{-\frac{1}{2}\sigma^2 \Omega^2} (Z_v - Z_s)\right) |01\rangle\langle 01|_{sv} \tag{C7}$$

$$+ \frac{P_v}{4} \left(1-Z_s Z_v - e^{-\frac{1}{2}\sigma^2 \Omega^2} (Z_v - Z_s)\right) |10\rangle\langle 10|_{sv} + \left(\frac{1-Z_s}{2}\right) P_v \left(\frac{1-Z_v}{2}\right) |11\rangle\langle 11|_{sv} + (1-P_V) \rho_s \otimes \tilde{\rho}_v \tag{C8}$$

which can be expressed in terms of the target cooling state as

$$\rho'_{\text{error}} = \rho' + P_v \frac{\left(1 - e^{-\sigma^2 \Omega^2/2}\right)}{2} \frac{(1 + Z_s) - (1 + Z_v)}{2} |01\rangle\langle 01| + P_v \frac{\left(1 - e^{-\sigma^2 \Omega^2/2}\right)}{2} \frac{(1 - Z_s) - (1 - Z_v)}{2} |10\rangle\langle 10| \quad (C9)$$

and similarly the reduced state of the system being cooled

$$\rho'_{\text{error}_s} = \rho'_s + P_v \frac{\left(1 - e^{-\sigma^2 \omega^2/2}\right)}{2} \frac{(1 + Z_s) - (1 + Z_v)}{2} |0\rangle\langle 0| + P_v \frac{\left(1 - e^{-\sigma^2 \Omega^2/2}\right)}{2} \frac{(1 - Z_s) - (1 - Z_v)}{2} |1\rangle\langle 1| \qquad (C10)$$

which allows us to obtain a relationship between normalised ground states as

$$r_{\text{error}} = P_v r_v + (1 - P_v) r_s + P_v \frac{\left(1 - e^{-\sigma^2 \Omega^2 / 2}\right)}{2} (r_s - r_v)$$
 (C11)

$$= P_v r_v (1-p) + (1 - P_v (1-p)) r_s$$
 (C12)

where  $p = \frac{\left(1 - e^{-\sigma^2\Omega^2/2}\right)}{2}$ . In this way we obtain a relationship with the same form as that presented in [20] with a modified probability  $\widetilde{P_v} = P_v(1-p)$ 

$$r_{\text{error}} = \widetilde{P_v} r_v + (1 - \widetilde{P_v}) r_s \tag{C13}$$

this allows us to generalise to the application of n repeated SWAP protocols with a refreshed virtual qubit at each step giving the recurrence relation

$$\frac{r_v - r_{\text{error}}^{(n)}}{r_v - r_s} = (1 - \widetilde{P_v})^n \tag{C14}$$

which implies

$$r_{\text{error}}^{(n)} = r_v - (r_v - r_s)(1 - P_v(1 - p))^n$$
(C15)

and in the asymptotic regime of infinite swaps  $n \to \infty$  we have that  $r_{\text{error}} \to r_v$  and the system qubit is cooled down to the temperature of the virtual qubit despite error in timekeeping.

In the case of perfect timekeeping,  $\sigma=0$  which gives p=0 and recovers the relationship from [20] whereas in the case that  $\sigma=\infty$  we have  $p=\frac{1}{2}$  in (C15) meaning that whilst terrible timekeeping still gets you to the state you wish to cool to asymptotically, it does of course take longer. Physically, this may be interpreted as imperfect timekeeping giving you access to at worst half the virtual qubit population to swap within a given operation instead of the total virtual qubit population. Thus it is this partial swapping which impedes the cooling, but in some sense something is always swapped in the right direction provided that the virtual qubit's virtual temperature is lower than that of the system qubit to begin with.

Whilst we are still able to cool a qubit to an arbitrary target temperature with an imperfect clock controlling our cooling protocol it is clear that one would require more resources to do so. To explore this, a rate of cooling within this context can be obtained by taking the central difference of the recurrence relation eq. (C15).

$$R_h = \frac{r_{\text{error}}^{(n+\frac{h}{2})} - r_{\text{error}}^{(n-\frac{h}{2})}}{h} \tag{C16}$$

for different values of p given by the variance of the tick distribution. Here h is the step of the finite difference. From eq. (C15) one finds the rate

$$R_h = \left(\frac{r_s - r_v}{h}\right) \left[ ((1 - \widetilde{P_v})^h - 1)(1 - \widetilde{P_v})^{n - \frac{h}{2}} \right]$$
 (C17)

which we plot in Fig 4 for fixed example values of  $r_s, r_v$  and  $P_v$  whilst varying  $\sigma$ . Showing that imperfect clocks require more SWAPs to cool to the target state.